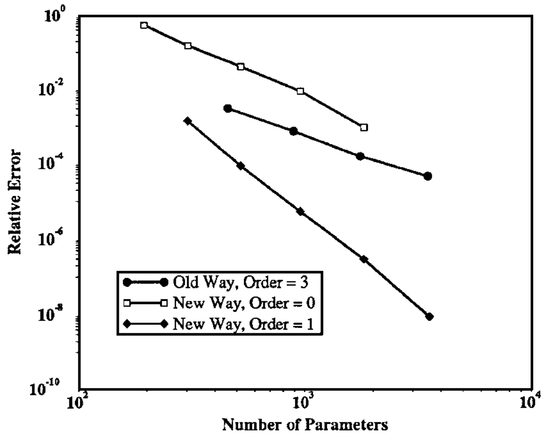

Fig. 3 Relative error in states and costates vs number of parameters, comparison of old and new ways.

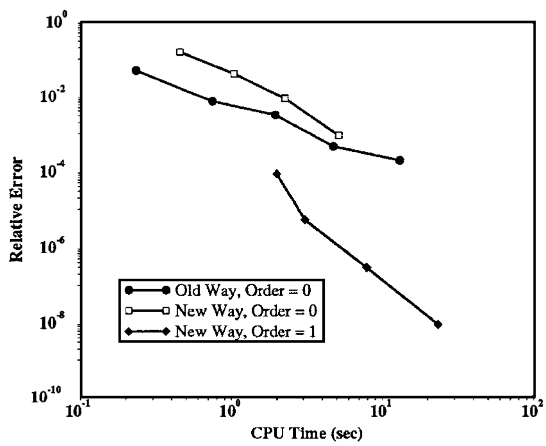

Fig. 4 Relative error in states and costates vs CPU time, comparison of old and new ways.

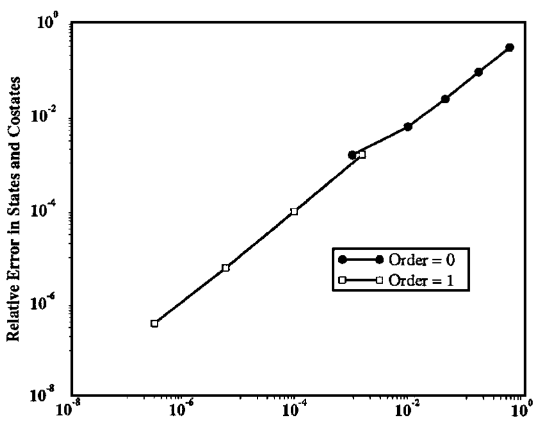

Fig. 5 Switching time accuracy vs overall accuracy.

three elements per phase as a starting point, with each data point corresponding to doubling the number of elements per phase.

Only the zeroth- and first-order shape function plots are shown for the new way, because the second-order shape function solution had zero error all along the time history, even for only two elements per phase. Although the CPU time necessary to implement the new method was higher for the zeroth-order shape functions than for the old way (reflecting the effect of the significantly increased size of the Jacobian), the multiple phase first-order solution is clearly far superior to the best results from the single-phase methodology. Thus, the key to solving this problem accurately and efficiently is clearly in the switching points, as seen in Fig. 5. Even for the three-element-per-phase solution with first-order shape functions, the switching times were all within 0.2% of the optimal value, moving an order of magnitude closer with each refinement. On the other hand, even with 192 elements obtained by uniform refinement and even with the highest-order shape functions, calculated switching times could get no closer than 0.2%.

VI. Conclusions

Two different methods have been illustrated to solve control-constrained optimal control problems using higher-order finite element formulations. In the first method, the optimal control problem is treated as if it had only one phase, with slack variables being used to enforce the control constraints. In the second method, the switching structure of the control constraints is specified ahead of time, and the problem is treated as a multiphase problem with unknown switching times.

The latter method proved to be much more accurate with the switching times being calculated explicitly, with a node point always being at a switching time. Results for a textbook problem show order of magnitude increases in accuracy using the second method, not only for a given number of parameters, but also for a given amount of CPU time.

References

[1]Warner, M. S., and Hodges, D. H.,"Solving Optimal Control Problems Using *hp*-Version Finite Elements in Time," *Journal of Guidance, Control, and Dynamics* (submitted for publication).

[2]Bryson, A. E., and Ho, Y.-C., *Applied Optimal Control—Optimization, Estimation, and Control*, Hemisphere, New York, 1975, Chap. 2.

[3]Hodges, D. H., and Hou, L.-J., "Shape Functions for Mixed *p*-Version Finite Elements in the Time Domain," *Journal of Sound and Vibration*, Vol. 145, No. 2, 1991, pp. 169–178.

[4]Bless, R. R., and Hodges, D. H., "Finite Element Solution of Optimal Control Problems with State-Control Inequality Constraints," *Journal of Guidance, Control, and Dynamics*, Vol. 15, No. 4, 1992, pp. 1029–1032.

Application of the Nyquist Stability Criterion on the Nichols Chart

Joseph C. Slater*
Wright State University, Dayton, Ohio 45435-0001

Introduction

THE classical implementation of the Nyquist stability criterion is well known. It is most often used as a stability check when eigenvalue analysis of a closed-loop system is not considered to be reliable, or when uncertainty exists in the plant. All that is necessary for determining stability of the closed-loop system is to know the number of poles on and to the right of the imaginary axis of the open-loop system as well as the frequency-response function. Although valuable as a stability check, it is difficult to use as a tool because loop shaping goals guide the control design process. In addition, the Nyquist stability criterion is generally defined on the open-loop Nyquist plot. This is not directly useful for design techniques based on the Nichols chart such as Quantitative Feedback Theory. Cohen et al.[1] have previously extended the Nyquist stability criterion to the Nichols chart. Here a simpler formulation is presented that provides the designer with additional insight useful in determining loop shaping goals for stable controller design. The formulation assists not only in stability analysis, but in prescribing design objectives for achieving stabilizing continuous control designs.

Received Jan. 14, 1998; revision received July 6, 1998; accepted for publication Oct. 6, 1998.

*Assistant Professor, Department of Mechanical and Materials Engineering. Member AIAA.

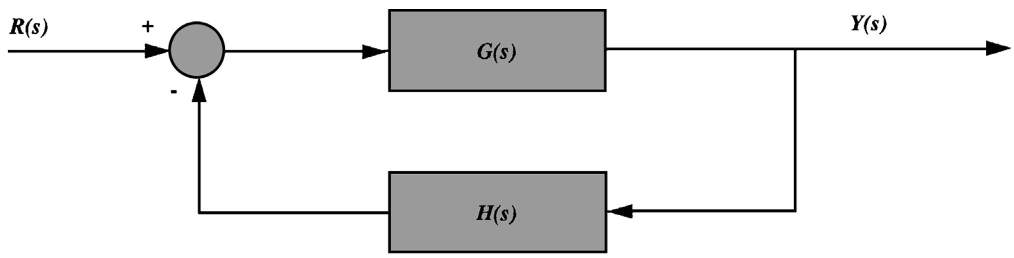

Fig. 1 Block diagram of basic feedback control system.

Theory

Because the open-loop Nyquist and Nichols plots can each be obtained from the other, it seems intuitive that, although the Nyquist stability criterion is based on the use of the Nyquist chart, one should be able to apply it using the Nichols chart. The following brief explanation shows how it can be done.

Consider a system defined by the block diagram of Fig. 1. The transfer function between $R(s)$ and $Y(s)$ is given by

$$\frac{Y(s)}{R(s)} = \frac{G(s)}{1+G(s)H(s)} = \frac{G(s)}{1+L(s)} \tag{1}$$

"The Nyquist criterion for stability of the closed-loop system is

$$\Phi = -(0.5P_\omega + P_{-1})180°\text{"} \tag{2}$$

(Ref. 2). Here P_ω is the number of poles of $L(s)$ on the imaginary axis and P_{-1} is the number of unstable poles of $L(s)$. The angle Φ (degrees) is the angle traversed by the Nyquist plot (counterclockwise) of $L(s)$ with respect to the $(-1, j0)$ point as $j\omega$ goes from ∞ to 0. Taking $j\omega$ from 0 to ∞ gives the negative expression.

Consider example 9-5 from Kuo's text.[2] It is a nonminimum phase system with a pole on the imaginary axis defined by the open-loop transfer function $L(s) = [K(s-1)/s(s+1)]$. For this example, $P_\omega = 1$ and $P_{-1} = 0$. Hence, the closed-loop stability requirement is

$$\Phi = -(0.5P_\omega + P_{-1})180 = -90 \tag{3}$$

Observing Fig. 2 for $K = 1$, one can see that the phasor drawn from the point $(-1, 0j)$ to the Nyquist plot of $L(s)$ traverses positive 90 deg as ω goes from ∞ to 0. Thus, the closed-loop system is unstable. In Fig. 2, one can see that the only value of K shown that results in the system being closed-loop stable is $K = -0.5$. The actual range of values of K for which the system is stable is $-1 < K < 0$.

Figure 3 shows the Nichols plot for the same system with the same three gains. The angle Φ can be found from the plots using the following guidelines. The positive direction along the open-loop plot is defined to go from $j\omega = 0$ to $j\omega = \infty$. These guidelines simply correlate similar parts of the Nichols and Nyquist charts to one another by noting that, once the magnitude of the open-loop transfer function is less than 0 dB (and remains below 0 dB), the angle traversed about the point $(-1, j0)$ on the Nyquist chart is zero. The final angle at high frequencies goes to 0 deg (or a multiple of 360 deg) assuming the magnitude decreases to 0 in the limit as $j\omega$ goes to ∞.

First, find the open-loop phase angle at $j\omega = 0$. Call this Φ_1. Second, find the phase angle (Φ_2) at the open-loop amplitude of 0 dB for the highest value of ω. From this point, go to the nearest open-loop phase of 0 deg or a multiple of 360 deg (positive or negative). Call this angle Φ_3. Make sure to use a multiple-sheet Nichols chart or keep track of how many times you pass through the plot from right to left. The angle Φ can be found by the equation

$$\Phi = \Phi_1 - \Phi_3 \tag{4}$$

For example, observing Fig. 3 for $K = 1$, the initial open-loop phase is $\Phi_1 = 90$ deg. This is found by unwrapping the Nichols chart so that the plot does not jump from one side of the graph to the other. When the open-loop magnitude is 0 dB (but never coming back over 0 dB), the open-loop phase is $\Phi_2 \approx 0$ deg. The nearest multiple of 360 or 0 deg is 0 deg. Thus, $\Phi_3 = 0$ deg and the total angle traversed is $\Phi_1 - \Phi_3 = 90$ deg. From Eq. (3), this system is unstable.

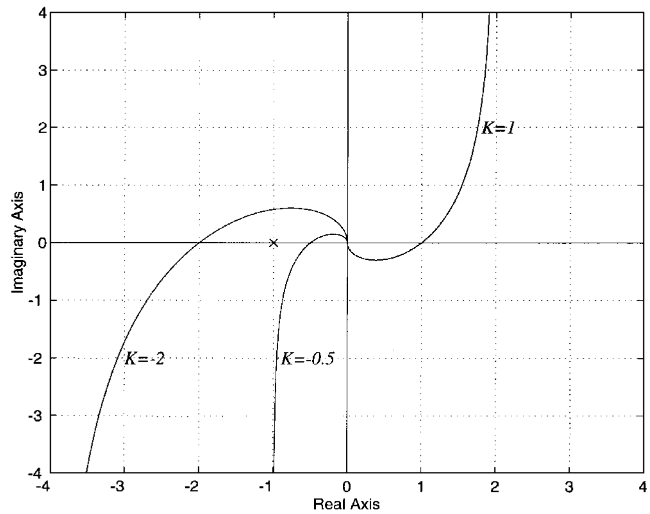

Fig. 2 Nyquist plots of $L(s) = [K(s-1)]/[s(s+1)]$.

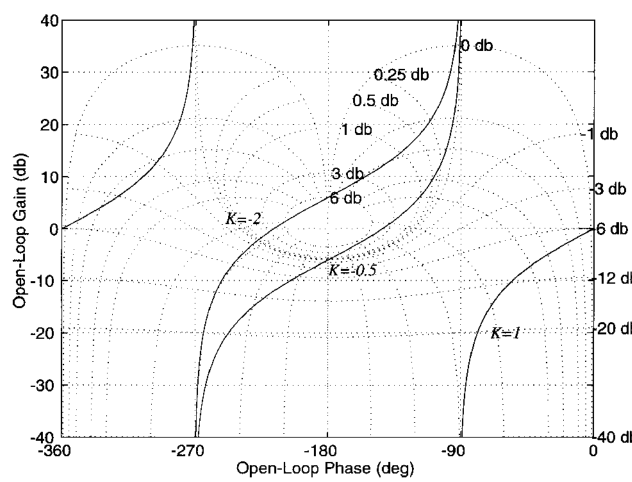

Fig. 3 Nichols plot of $L(s) = [K(s-1)]/[s(s+1)]$.

Observing Fig. 3 for $K = -0.5$, the initial open-loop phase is $\Phi_1 = -90$ deg. When the open-loop magnitude is 0 dB, the open-loop phase is $\Phi_2 \approx -135$ deg. The nearest multiple of 360 or 0 deg is again 0 deg itself. Thus, $\Phi_3 = 0$ deg, and the total angle traversed is $\Phi_1 - \Phi_3 = -90$ deg. From Eq. (3), this system is stable.

Observing Fig. 3 again for $K = -2$, the initial open-loop phase is $\Phi_1 = -90$ deg. When the open-loop magnitude is 0 dB, the open-loop phase is $\Phi_2 \approx -225$ deg. The nearest multiple of 360 or 0 deg is -360 deg. Thus, $\Phi_3 = -360$ deg, and the total angle traversed is $\Phi_1 - \Phi_3 = -90 + 360 = 270$ deg. From Eq. (3), this system is unstable.

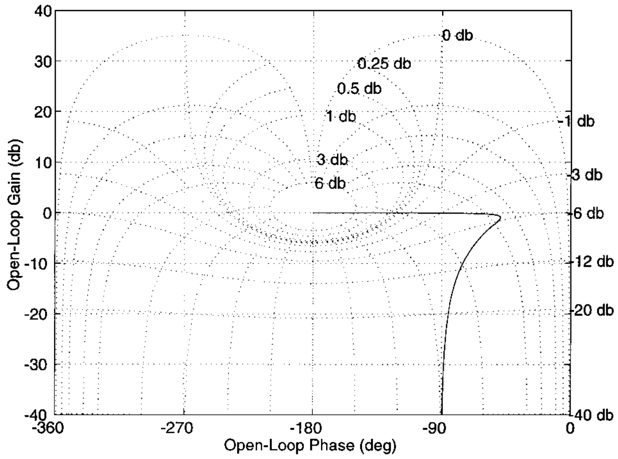

Fig. 4 Example 2, stabilizing an unstable system [$L(s) = K(s + 1)/(s^2 + 9s - 10)$], where $K = 10$.

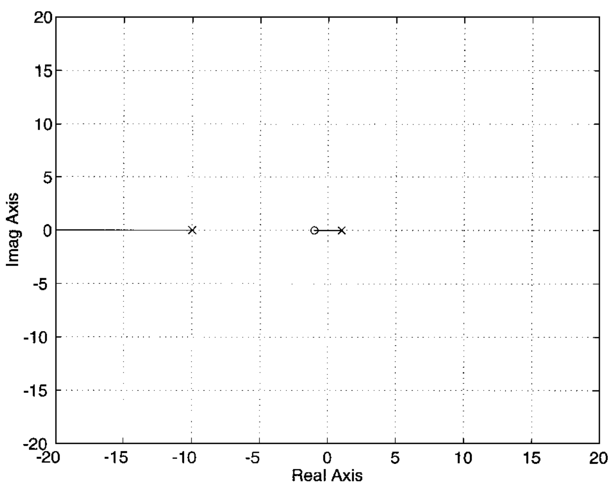

Fig. 5 Root locus of $L(s) = K(s + 1)/(s^2 + 9s - 10)$.

Consider a second example with one unstable pole. The objective here is to determine how to modify the open-loop transfer function so that the closed-loop transfer function will be stable. The open-loop transfer function is given by $L(s) = K(s+1)/(s^2 + 9s - 10)$. Equation (2) states $\Phi = -(0.5P_\omega + P_{-1})180$ deg must be true for the system to be stable. The open-loop poles are -10 and 1. Because there are no poles on the imaginary axis and there is one unstable pole, $P_\omega = 0$ and $P_{-1} = 1$. Thus, for a stable closed-loop system, we require that $\Phi = -180$ deg. The Nichols plot of $L(s)$ is shown in Fig. 4 for a gain of $K = 10$. The initial phase at $\omega = 0$ is $\Phi_1 = -180$ deg. Of course, this is only true if the gain is raised slightly such that the initial magnitude is greater than 0 dB. If $K = 0$, the initial phase is not defined by this technique. If $K < 10$, then $\Phi_1 = -180$ deg because for $s < 0$ the 0 dB crossing is nearest 360 deg. The nearest multiple of 360 deg when the magnitude of $L(s)$ is 0 dB is 0 deg. Thus, if the gain is greater than 10, then $\Phi_1 - \Phi_3 = -180 + 0 = -180$ deg as required for stability. The root locus of Fig. 5 shows this to be the case.

Conclusions

A simple method for applying Nyquist's stability criterion on the Nichols Chart has been presented. The approach is applicable to open-loop systems with poles and/or zeros in the right-half plane. The result is a method for evaluating not only the stability of existing controlled systems, but also for determining control design objectives on the Nichols chart.

References

[1]Cohen, N., Chait, Y., Yaniv, O., and Borghesani, C., "Stability Analysis Using Nichols Charts," *International Journal of Robust and Nonlinear Control*, Vol. 4, No. 2, 1994, pp. 3–20.

[2]Kuo, B. C., *Automatic Control Systems*, 7th ed., Prentice–Hall, New York, 1991, Chap. 9.

Optimal Control and Filtering for Nonstandard Singularly Perturbed Linear Systems

Vojislav Kecman*
University of Auckland, Auckland 1, New Zealand
and
Zoran Gajic†
Rutgers University, Piscataway, New Jersey 08855

Introduction

A POWERFUL algorithm for the exact slow–fast decomposition of the algebraic Riccati equation of standard singularly perturbed systems is developed in Ref. 1, so that the optimal control and filtering tasks can be solved exactly and performed independently in slow and fast time scales.[2,3] In this Note, we show that the same algorithm, under the appropriate assumptions is applicable to the algebraic Riccati equation of nonstandard singularly perturbed control systems (having singular fast subsystem matrix). Nonstandard singularly perturbed systems are the modern research trend in control theory of singular perturbations.[4–9] The result obtained for the decomposition of the algebraic Riccati equation is used in this Note to obtain the exact pure-slow and pure-fast decomposition of optimal control and filtering tasks of nonstandard singularly perturbed linear systems. Note that in the control literature only approximate results for nonstandard singularly perturbed systems are available.

Before the results of Ref. 1 were available, control engineers were able to decompose exactly only linear singularly perturbed systems by using the celebrated Chang transformation.[10] In Ref. 11 the nonlinear algebraic Riccati equation was decomposed into slow and fast algebraic Riccati equations with the accuracy of $\mathcal{O}(\epsilon)$, where ϵ is a small positive singular perturbation parameter. Several real-world examples done in Refs. 2 and 12–14 indicate that very often an $\mathcal{O}(\epsilon)$ order of accuracy is not satisfactory. The results of Ref. 1 are, as a matter of fact, the extended and improved results of Ref. 11. It can be said that the results of Ref. 1 achieve the same goal as the results of Ref. 11, but with perfect accuracy.

The goal of this Note is to show that the results developed in Ref. 1 and the related work of Ref. 3 can be extended to nonstandard singularly perturbed systems. It should be pointed out that mechanical control systems in the modal coordinates[15] displaying slow and fast time scales are nonstandard singularly perturbed linear control systems—e.g., the linearized model of a flexible space structure.[16]

Conditions under which the first approximation of nonstandard singularly perturbed control systems can be studied are established in Ref. 8. It is important to point out that the results of Ref. 8 produce the $\mathcal{O}(\epsilon)$ accuracy only. In contrast, the results of this Note produce the exact solution and preserve the slow–fast decomposition features of Ref. 8.

Optimal Control of Nonstandard Singularly Perturbed Linear Systems

A nonstandard singularly perturbed control linear system is represented by

$$
\begin{aligned}
\dot{x}_1(t) &= A_1 x_1(t) + A_2 x_2(t) + B_1 u(t) \\
\epsilon \dot{x}_2(t) &= A_3 x_1(t) + A_4 x_2(t) + B_2 u(t)
\end{aligned}
\tag{1}
$$

Received April 6, 1998; revision received Sept. 1, 1998; accepted for publication Oct. 9, 1998.

*Senior Lecturer, Department of Mechanical Engineering.

†Associate Professor, Department of Electrical and Computer Engineering.